

Received March 25, 2021, accepted April 15, 2021, date of publication April 19, 2021, date of current version April 28, 2021.

Digital Object Identifier 10.1109/ACCESS.2021.3074009

A Hybrid Companding and Clipping Scheme for PAPR Reduction in OFDM Systems

ZHITONG XING¹, KAIMING LIU¹, (Member, IEEE),
ADITYA S. RAJASEKARAN^{2,3}, (Member, IEEE), HALIM YANIKOMEROGU², (Fellow, IEEE),
AND YUANAN LIU¹, (Member, IEEE)

¹School of Electronic Engineering, Beijing University of Posts and Telecommunications, Beijing 100086, China

²Department of Systems and Computer Engineering, Carleton University, Ottawa, ON K1S 5B6, Canada

³Ericsson Canada Inc, Ottawa, ON K1S 5B6, Canada

Corresponding author: Kaiming Liu (kmlu@bupt.edu.cn)

This work was supported in part by the Science and Technology Key Project of Guangdong Province, China, under Grant 2019B010157001, in part by the National Natural Science Foundation of China under Grant 61821001, and in part by the Discovery Grant of the Natural Sciences and Engineering Research Council of Canada. The work of Aditya S. Rajasekaran was supported by the Ericsson Canada Inc., in the form of tuition assistance.

ABSTRACT Orthogonal frequency division multiplexing (OFDM) continues to be deployed in 5G communication systems and is likely to be used in beyond 5G (B5G) communication systems as well, due to its many advantages. However, one major drawback with OFDM systems is its high peak-to-average power ratio (PAPR), especially with large bandwidth transmissions. In this paper, we have provided a regularization optimization based flexible hybrid companding and clipping scheme (ROFHCC) used for PAPR reduction in OFDM systems. To reduce the design complexity, the companding function has two parts. It restrains the signal samples with amplitudes over a given value to a constant value for both peak power reduction and small power compensation. For signals with samples less than a given amplitude, they are expanded by a linear companding function. We build a regularization optimization model to jointly optimize the companding distortion as well as the continuity of the companding function for bit error rate (BER) performance as well as power spectral density (PSD) performance. Simulation results indicate that for the same PAPR performance, the proposed companding scheme has an advantage over the referenced companding schemes. For example, when the average signal power is normalized to be 1, we choose both PAPR for ROFHCC scheme and two-piecewise companding (TPWC) scheme as 4 dB, then we can find that at $BER = 10^{-4}$, the minimum required E_b/N_0 for ROFHCC scheme is around 2.3 dB lower than TPWC scheme.

INDEX TERMS OFDM, PAPR, companding, distortion.

I. INTRODUCTION

Orthogonal frequency division multiplexing (OFDM) has been extensively used in a number of wireless communication standards because of its high spectral efficiency, robustness to multipath fading effects and low implementation complexity. However, despite its advantages, one of the inherent drawbacks of OFDM systems is its high peak-to-average power ratio (PAPR) [1]. A high PAPR causes a large signal distortion when the signals pass through a high power amplifiers (PAs) at the transmitter end. As a result, addressing the PAPR problem has been widely studied in OFDM systems [2], through different solutions that involve tradeoffs between

the level of PAPR reduction achieved and the cost of either additional complexity or bit error rate (BER) loss or both. These tradeoffs in the solutions addressing the PAPR problem become even more critical in 5G and beyond 5G (B5G) systems that are expected to support a variety of end user devices, from low-cost sensors to high-end smart phones and virtual reality goggles. Each of these transmitting devices in the uplink come with PAs that have different levels of tolerance to the PAPR, depending typically on the cost of the PAs in the device [3]. Another consideration with B5G systems is the use of large bandwidth carriers, particularly in the mmWave spectrum which leads to carriers with a large number of OFDM sub-carriers. Applying PAPR reduction techniques that scale in complexity with the number of subcarriers becomes challenging in such an environment.

The associate editor coordinating the review of this manuscript and approving it for publication was Yue Zhang¹.

Furthermore, with novel multiple access solutions, e.g., non-orthogonal multiple access (NOMA), that run over OFDM being studied for 5G systems, these tradeoffs in the PAPR solutions between PAPR reduction, complexity and BER loss are an important research topic [4].

As outlined by the survey in [2], several techniques that reduce the PAPR in OFDM systems have been proposed in the literature. Broadly, they can be classified into three main categories: multiple signaling and probabilistic techniques, coding techniques and lastly signal distortion techniques. In the first category of multiple signaling and probabilistic techniques, the goal is to reduce the probability of transmitting a signal of high PAPR by generating several candidate signals and transmitting the one with least PAPR. Common techniques in this category include selective mapping [5] and partial transmit sequences [6]. The second class of PAPR reduction method involve the coding techniques. Codes used for error detection and correction, such as linear block code, Golay sequences, and polar codes [7] have all been used to perform PAPR reduction. However, both these classes of PAPR reduction techniques require large computation complexity, which may not be suitable when the number of subcarriers is large. A third category of PAPR reduction techniques, called signal distortion techniques in [2], involves introducing in-band and out-of-band distortion to the transmitted signal to achieve PAPR reduction. These techniques do not introduce any complexity overhead, but the distortion introduced impacts the BER performance adversely. The goal then is to find an acceptable tradeoff between the PAPR reduction achieved and the additional BER loss incurred. The most common of these signal distortion techniques is clipping, where peaks in the signal above a certain threshold are clipped to control the peak instantaneous power in the signal. One of the more advanced techniques in this category of PAPR reduction techniques is that of companding, which is the focus of this paper.

Companding schemes can be broadly divided into linear and non-linear companding schemes. Among the linear schemes, the authors in [8] and [9] provided linear companding functions with several inflection points and a different signal amplitude was companded with different scales. In [10], to maintain the average signal power constant along with a one-to-one mapping, the discussed two-piece companding scheme (TPWC) scales a small signal amplitude, while a large signal amplitude is addressed through both scaling and shifting. However, the TPWC scheme does not employ clipping and thus cannot reduce the PAPR effectively. Also, in [11], authors proposed a piecewise linear companding (PLC) scheme that employed minimum mean square error to set the parameters of the companding function. In the second category, nonlinear companding functions are used to reduce the PAPR of OFDM signals. In [12], Wang first proposed the μ -law companding (MC) scheme and the bit error rate (BER) performance was introduced in [13]. However, the MC scheme reduces PAPR at the expense of an increase in the average signal power. Later, literatures

[14]–[16] represented by exponential companding (EC) scheme first assigned an ideal probability density function (PDF) with low PAPR, and then the nonlinear companding function is found based on the original signal PDF and assigned signal PDF. In other work [14], a modification of MC, called “root-based MC” (RMC), was provided. It used μ -law to compand the d th root of the amplitude of OFDM signal. After μ -law companding, the power compensation method was implemented to make the signal power before and after companding be at the same level. Recently, [17] provided amplitude limiting companding (ALC) scheme, which used polynomials to compress the signal amplitude. In [18], the authors proposed a hybrid clipping and companding scheme for PAPR reduction in OFDM systems. The signals will first pass through the clipping operator, and then the authors use companding function to further reduce the PAPR. In [19], the authors have proposed a hybrid of clipping and companding (HCC) scheme. It clips high amplitude signals and expands low amplitude signals. However, this scheme cannot guarantee the average signal power constant, which leads to a relatively high energy consumption.

In this paper, We have provided a regularization optimization based flexible hybrid companding and clipping (ROFHCC) scheme for PAPR reduction in OFDM systems. In the proposed companding scheme, signals with amplitudes over a given segment point are restrained to a determined clipping value. The signals with amplitudes less than the segment point are amplified for power compensation by an expanding function. When the peak power restriction is determined, we build the variation problem aimed at companding distortion minimization to find the expanding function. According to Euler–Lagrange equation, the lowest companding distortion expanding function is linear function. The main contributions of our paper are two-fold. First, we notice that the HCC scheme is also an optimal form for proposed companding scheme but without average power constant. So, we provide MHCC scheme, which consider the average power constant. Here we consider the constraint condition of constant average power of OFDM signals, which is much useful for practical implementations. Actually, if the change of signal power is not negligibly small, the high PAs’ gain must be dynamically adjusted, which will increase the hardware cost. [2]. In addition, signals with increased power may traverse the nonlinear region of high PAs, leading to larger distortions and degradation of BER performance. Second, we build a regularization optimization problem to find optimal clipping value as well as slope value for our companding function. The optimization goal is the combination of companding distortion as well as the continuity for proposed companding scheme while the constraint condition is the average signal power constant before and after companding. And we give analytical solutions for some cases.

The rest of this work is organized as follows. In Section II, we introduce the OFDM system model along with a characterization of PAPR. In Section III, the proposed companding function is detailed where the variation method is used to find

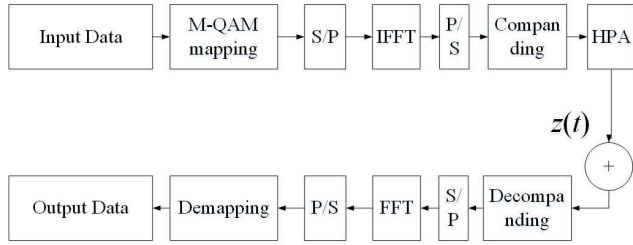


FIGURE 1. Block diagram of OFDM modulation systems.

the optimal expanding function by minimizing signal distortion. We also build regularization optimization problems with constraint conditions and give analytical solutions in some cases and in Section IV, simulation results comparing the proposed scheme to other similar schemes from the literature are provided. Finally, some concluding remarks are made in Section V.

II. OFDM SYSTEM MODEL

The general OFDM transmission system is shown in Fig. 1. Let $X_k, k \in \{0, 1, 2, \dots, N - 1\}$ represents the complex modulated symbols to be transmitted in an OFDM symbol with N subcarriers. After Inverse Fast Fourier Transform (IFFT), the time-domain OFDM symbol is

$$x_n = \frac{1}{\sqrt{N}} \sum_{k=0}^{N-1} X_k e^{j2\pi \frac{kn}{N}}. \tag{1}$$

Based on the central limit theorem, the real and imaginary parts of the OFDM signal in the time domain can be approximated by a complex Gaussian distribution when N is large enough [17]. This implies that the amplitude of the signal $|x_n|$ obeys the Rayleigh distribution with the PDF as

$$f(x) = \frac{2x}{\sigma^2} e^{-\frac{x^2}{\sigma^2}}, \tag{2}$$

where σ^2 is the variance of $|x_n|$. The cumulative distribution function (CDF) of the Rayleigh distribution is

$$F(x) = 1 - e^{-\frac{x^2}{\sigma^2}}. \tag{3}$$

In OFDM transmission, PAPR is defined as the ratio between the maximum instantaneous power and the average power of the signal in one symbol period. Hence, the PAPR of the OFDM transmitted signal can be expressed as

$$PAPR = \frac{\max_{0 \leq n \leq N-1} |x_n|^2}{E(|x_n|^2)}. \tag{4}$$

The PAPR statistics using the complementary cumulative distribution function (CCDF), offer more meaningful insights by estimating the probability of PAPR exceeding a desired target. Most of the PAPR reduction techniques are evaluated using the CCDF metric, denoted as $CCDF_{PAPR}(\gamma)$,

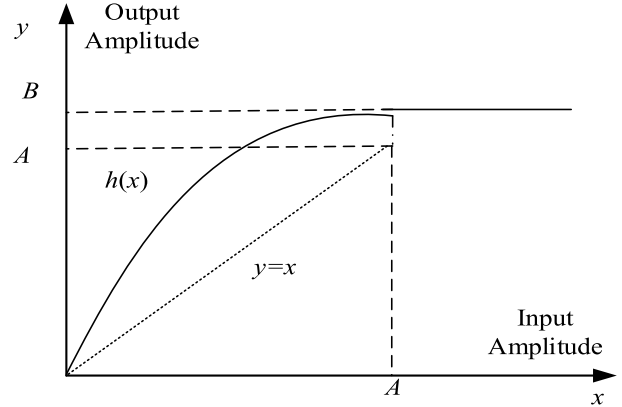


FIGURE 2. Design of companding function.

and given by

$$CCDF_{PAPR}(\gamma) = 1 - P\left\{\frac{|x|^2}{\sigma^2} \leq \gamma\right\}^N = 1 - (1 - e^{-\gamma})^N. \tag{5}$$

III. PROPOSED COMPANDING SCHEME

The proposed companding function is shown in Fig. 2. When the original signal amplitude is less than the given peak amplitude, an expanding function, $h(x)$, is used to enlarge the signal amplitude. When the original signal amplitude is larger than the given peak amplitude, the signal amplitude will be restrained to a constant value B . Thus, for the n th OFDM signal sample, the companding function can be written as

$$y(x_n) = \text{sign}(x_n) \begin{cases} h(|x_n|), & |x_n| \leq A, \\ B, & |x_n| > A. \end{cases} \tag{6}$$

where A is the segmentation point. The segmentation point means the piecewise point. And the argument of the piecewise function needs to bring in a new expression from this point on. Then the average companding distortion is

$$\begin{aligned} \sigma_c^2 &= E(\sigma_x^2) \\ &= \int_0^A \{[h(x) - x]^2 f(x)\} dx + \int_A^{+\infty} [(B - x)^2 f(x)] dx. \end{aligned} \tag{7}$$

Eqn. (7) shows that with pre-determined values of A and B , σ_c^2 varies with expanding function $h(x)$.

To keep the input and output of the proposed companding function at the same average power level, the companding function should satisfy the condition

$$\int_0^{\infty} y^2(x) f(x) dx = \int_0^A h^2(x) f(x) dx + \int_A^{+\infty} B^2 f(x) dx = \sigma^2. \tag{8}$$

Therefore, we formulate the problem of solving $h(x)$ as an optimization problem to mitigate companding distortion

$$\begin{aligned} & \arg \min_{h(x) \in C_n} \sigma_c^2, \\ & \text{s.t.} \int_0^A h^2(x) f(x) dx + \int_A^{+\infty} B^2 f(x) dx = \sigma^2. \end{aligned} \quad (9)$$

The optimization problem proposed in eqn. (9) is solved based on the Euler–Lagrange function [20] in Appendix-A. We also prove the sufficiency of the Euler–Lagrange function in solving this problem in Appendix-B. Based on these results, the optimized expanding part function, $h(x)$, can be expressed as

$$h(x) = kx. \quad (10)$$

Thus, the optimal companding function is given as

$$y(x_n) = \text{sign}(x_n) \begin{cases} k|x_n|, & |x_n| \leq A, \\ B, & |x_n| > A. \end{cases} \quad (11)$$

Considering that the probability the signals need clipping is related with the segmentation point A , which is given as

$$\Pr\{|x_n| > A\} = \int_A^{+\infty} \frac{2x}{\sigma^2} e^{-\frac{x^2}{\sigma^2}} dx = e^{-\frac{A^2}{\sigma^2}}. \quad (12)$$

According to eqn. (12), we can find that with the increasing of segmentation point A , the probability that the signals need clipping will decreasing.

Fig. 3 shows the relationship between A and the probability that the signals need clipping when the average signal power σ^2 is normalized to be 1. From Fig. 3, we can find that with the increasing of A , the probability that the signals need clipping decreases sharply. Furthermore, when A is larger than 1.5, the probability that the signals need clipping is less than 10^{-1} . So we can find that the clipping has a relatively small influence on the BER and power spectral density (PSD) performance of the signals. This means that the proposed companding schemes seem to perform better than other existing methods since the proposed companding schemes use clipping for peak power reduction. And linear companding is applied for power compensation. In fact, linear companding is beneficial for reducing signal distortion, which can improve the BER and PSD performance. Clipping will cause signal distortion, but considering that the probability the signals need clipping is small enough, so the BER and PSD performance influence caused by clipping is limited.

Considering that the companding function cannot change the average signal power before and after companding, we get

$$\int_0^A (kx)^2 f(x) dx + \int_A^{+\infty} B^2 f(x) dx = \sigma^2. \quad (13)$$

This means that

$$k^2 \sigma^2 - k^2 e^{-\frac{A^2}{\sigma^2}} (A^2 + \sigma^2) + B^2 e^{-\frac{A^2}{\sigma^2}} = \sigma^2. \quad (14)$$

By solving eqn. (14), we obtain that

$$k = \sqrt{\frac{\sigma^2 - B^2 e^{-\frac{A^2}{\sigma^2}}}{\sigma^2 - e^{-\frac{A^2}{\sigma^2}} (A^2 + \sigma^2)}}. \quad (15)$$

To make the square root in eqn. (15) be meaningful, it should satisfy

$$\left(\sigma^2 - B^2 e^{-\frac{A^2}{\sigma^2}}\right) \left[\sigma^2 - e^{-\frac{A^2}{\sigma^2}} (A^2 + \sigma^2)\right] > 0. \quad (16)$$

In Appendix C, we will prove that

$$\sigma^2 - e^{-\frac{A^2}{\sigma^2}} (A^2 + \sigma^2) > 0. \quad (17)$$

So we obtain

$$\sigma^2 - B^2 e^{-\frac{A^2}{\sigma^2}} > 0. \quad (18)$$

Thus, with a determined of A , we should satisfy that

$$B < \sigma \sqrt{e^{\frac{A^2}{\sigma^2}}}. \quad (19)$$

Thus, the proposed companding scheme is applied by carefully selecting parameters A and B such that they satisfy eqn. (18). Then, using A and B as input, k is set according to eqn. (15). The expanding part function $h(x)$, is then set as a linear amplification function, $h(x) = kx$. The signals with amplitudes over a given segmentation point are clipped for both peak power reduction and average signal power compensation. The signals with amplitudes lower than the segmentation point are expanded with linear amplification function.

A. MODIFICATION OF HCC

Based on our conclusion given in eqn. (11), we can find that HCC scheme is a special case of our companding function. It is given as

$$y(x_n) = \text{sign}(x_n) \begin{cases} \frac{A|x_n|}{\sigma \eta^*}, & |x_n| \leq \eta^* \sigma, \\ A, & |x_n| > \eta^* \sigma. \end{cases} \quad (20)$$

However, HCC scheme cannot guarantee the average signal power constant. This will make the high PAs dynamically adjust the signal power, which increase the hardware cost. We then provide a modification of HCC scheme (MHCC), which can guarantee the signal power before and after companding be constant. The appropriate value of η^* is given as

$$\frac{A^2}{\eta^{*2}} \int_0^{\eta^*} x^2 \frac{2x}{\sigma^2} e^{-\frac{x^2}{\sigma^2}} dx + \frac{A^2}{\eta^{*2}} \int_{\eta^*}^{+\infty} A^2 \frac{2x}{\sigma^2} e^{-\frac{x^2}{\sigma^2}} dx = \sigma^2. \quad (21)$$

By expanding the integral equation in eqn. (21), we can obtain that

$$\frac{A^2}{\eta^{*2} \sigma^2} \left[\sigma^2 - e^{-\eta^{*2}} (\sigma^2 + e^{-\eta^{*2}}) \right] + A^2 e^{-\eta^{*2}} = \sigma^2. \quad (22)$$

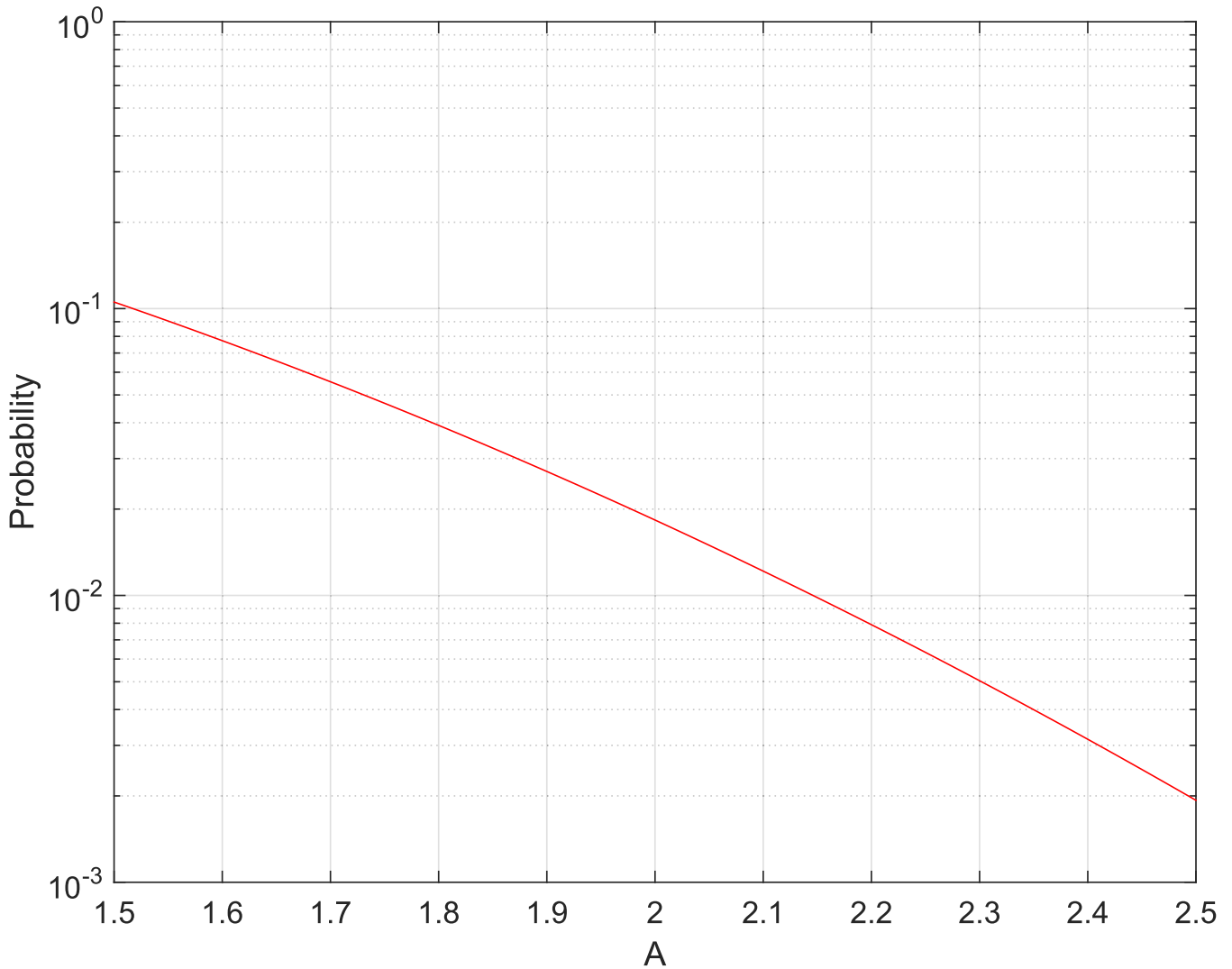


FIGURE 3. Relationship between A and probability.

By solving eqn.(22), we obtain

$$A = \sqrt{\frac{\eta^{*2}\sigma^4}{\eta^{*2}\sigma^2 e^{-\eta^{*2}} + [\sigma^2 - e^{-\eta^{*2}}(\sigma^2 + e^{-\eta^{*2}})]}}. \quad (23)$$

B. A FLEXIBLE HYBRID COMPANDING AND CLIPPING SCHEME

MHCC scheme can guarantee the average signal power constraint, but cannot make the companding distortion be the lowest. In this part, we provide flexible hybrid companding and clipping (FHCC) scheme. According to eqn. (11), we can calculate the companding distortion given as

$$\begin{aligned} \sigma_c^2 &= \int_0^A (kx - x)^2 \frac{2x}{\sigma^2} e^{-\frac{x^2}{\sigma^2}} dx + \int_A^{+\infty} (B - x)^2 \frac{2x}{\sigma^2} e^{-\frac{x^2}{\sigma^2}} dx \\ &= (k - 1)^2 \left[\sigma^2 - e^{-\frac{A^2}{\sigma^2}} (A^2 + \sigma^2) \right] + B\sqrt{\pi}\sigma \operatorname{erf}\left(\frac{A}{\sigma}\right) \\ &\quad - B\sqrt{\pi}\sigma + e^{-\frac{A^2}{\sigma^2}} \left[(A - B)^2 + \sigma^2 \right]. \end{aligned} \quad (24)$$

Further, the companding function should satisfy the average signal power constant shown in eqn. (13). So for any given value of A, we can find the optimal value of k and B with the least companding distortion, under the constraint of average signal power constant. It is given as

$$\begin{aligned} &\min_{k,B} \sigma_c^2, \\ &\text{subject to } k^2\sigma^2 - k^2 e^{-\frac{A^2}{\sigma^2}} (A^2 + \sigma^2) \\ &\quad + B^2 e^{-\frac{A^2}{\sigma^2}} = \sigma^2. \end{aligned} \quad (25)$$

We can find the optimal value of k and B with Lagrange multiplier method. It is given as

$$H = \sigma_c^2 + \lambda \left[k^2\sigma^2 - k^2 e^{-\frac{A^2}{\sigma^2}} (A^2 + \sigma^2) + B^2 e^{-\frac{A^2}{\sigma^2}} - \sigma^2 \right]. \quad (26)$$

By expanding eqn. (26), we can obtain

$$\begin{aligned}
 H = & (k - 1)^2 \left[\sigma^2 - e^{-\frac{A^2}{\sigma^2}} (A^2 + \sigma^2) \right] \\
 & + B\sqrt{\pi}\sigma \operatorname{erf}\left(\frac{A}{\sigma}\right) - B\sqrt{\pi}\sigma + e^{-\frac{A^2}{\sigma^2}} \left[(A - B)^2 + \sigma^2 \right] \\
 & + \lambda \left[k^2\sigma^2 - k^2e^{-\frac{A^2}{\sigma^2}} (A^2 + \sigma^2) + B^2e^{-\frac{A^2}{\sigma^2}} - \sigma^2 \right]. \tag{27}
 \end{aligned}$$

To find the optimal value, we should solve the partial derivative equations given as

$$\begin{cases} \frac{\partial H}{\partial B} = 0, \\ \frac{\partial H}{\partial k} = 0, \\ \frac{\partial H}{\partial \lambda} = 0. \end{cases} \tag{28}$$

By expanding eqn. (28), we can obtain

$$2\lambda B e^{-\frac{A^2}{\sigma^2}} - 2(A - B) e^{-\frac{A^2}{\sigma^2}} - \sqrt{\pi}\sigma + \sqrt{\pi}\sigma \operatorname{erf}\left(\frac{A}{\sigma}\right) = 0, \tag{29}$$

$$2 \left[\sigma^2 - e^{-\frac{A^2}{\sigma^2}} (A^2 + \sigma^2) \right] (k\lambda + k - 1) = 0, \tag{30}$$

and

$$B^2 e^{-\frac{A^2}{\sigma^2}} + k^2 \left[\sigma^2 - e^{-\frac{A^2}{\sigma^2}} (A^2 + \sigma^2) \right] = \sigma^2. \tag{31}$$

According to eqn. (31), we obtain

$$k = \sqrt{\frac{\sigma^2 - B^2 e^{-\frac{A^2}{\sigma^2}}}{\sigma^2 - (A^2 + \sigma^2) e^{-\frac{A^2}{\sigma^2}}}}. \tag{32}$$

According to eqn. (30), we obtain

$$k = \frac{1}{1 + \lambda}. \tag{33}$$

By combining eqn. (32) and eqn. (33), we obtain

$$\lambda + 1 = \sqrt{\frac{\sigma^2 - (A^2 + \sigma^2) e^{-\frac{A^2}{\sigma^2}}}{\sigma^2 - B^2 e^{-\frac{A^2}{\sigma^2}}}}. \tag{34}$$

Further, according to eqn. (III-B), we can find

$$\lambda = \frac{2(A - B) e^{-\frac{A^2}{\sigma^2}} + \sqrt{\pi}\sigma - \sqrt{\pi}\sigma \operatorname{erf}\left(\frac{A}{\sigma}\right)}{2B e^{-\frac{A^2}{\sigma^2}}}. \tag{35}$$

According to eqn. (34) and eqn. (35), we obtain

$$\begin{aligned}
 & \sqrt{\frac{\sigma^2 - (A^2 + \sigma^2) e^{-\frac{A^2}{\sigma^2}}}{\sigma^2 - B^2 e^{-\frac{A^2}{\sigma^2}}}} \\
 & = \frac{2Ae^{-\frac{A^2}{\sigma^2}} + \sigma\sqrt{\pi} - \sigma\sqrt{\pi}\operatorname{erf}\left(\frac{A}{\sigma}\right)}{2Be^{-\frac{A^2}{\sigma^2}}}. \tag{36}
 \end{aligned}$$

By squaring eqn. (36), we can obtain

$$\begin{aligned}
 & \frac{\sigma^2 - (A^2 + \sigma^2) e^{-\frac{A^2}{\sigma^2}}}{\sigma^2 - B^2 e^{-\frac{A^2}{\sigma^2}}} \\
 & = \frac{\left[2Ae^{-\frac{A^2}{\sigma^2}} + \sigma\sqrt{\pi} - \sigma\sqrt{\pi}\operatorname{erf}\left(\frac{A}{\sigma}\right) \right]^2}{\left(2Be^{-\frac{A^2}{\sigma^2}} \right)^2}. \tag{37}
 \end{aligned}$$

Let

$$L = \sigma^2 - (A^2 + \sigma^2) e^{-\frac{A^2}{\sigma^2}} \tag{38}$$

and

$$M = \left[2Ae^{-\frac{A^2}{\sigma^2}} + \sigma\sqrt{\pi} - \sigma\sqrt{\pi}\operatorname{erf}\left(\frac{A}{\sigma}\right) \right]^2, \tag{39}$$

we can find

$$\frac{L}{\sigma^2 - B^2 e^{-\frac{A^2}{\sigma^2}}} = \frac{M}{\left(2Be^{-\frac{A^2}{\sigma^2}} \right)^2}. \tag{40}$$

Then we obtain

$$B = \sqrt{\frac{M\sigma^2}{Me^{-\frac{A^2}{\sigma^2}} + 4Le^{-2\frac{A^2}{\sigma^2}}}}. \tag{41}$$

C. REGULARIZATION OPTIMIZATION BASED FLEXIBLE HYBRID COMPANDING AND CLIPPING SCHEME

Besides the companding distortion, another important factor to be considered for companding function design is its continuity. The better the continuity performance is, the better the PSD performance for proposed companding scheme. We thus provide a regularization optimization based flexible hybrid companding and clipping scheme (ROFHCC). The general optimization scheme is given as

$$\begin{aligned}
 & \min_{k,B} \eta\sigma_c^2 + (1 - \eta) (B - kA)^2, \\
 & \text{subject to } k^2\sigma^2 - k^2e^{-\frac{A^2}{\sigma^2}} (A^2 + \sigma^2) + B^2e^{-\frac{A^2}{\sigma^2}} = \sigma^2. \tag{42}
 \end{aligned}$$

It is hard to find the analytical value for eqn. (42), but we can find numerical value for the eqn. (42). As an example, when $\sigma^2 = 1$, the optimal value for B and k with a given A and given η are given in Table I. We should notice that MHCC scheme is a special case for ROFHCC scheme with $\eta = 0$ while FHCC scheme is a special case with $\eta = 1$. We can flexibly adjust the parameter η to give a balance between companding distortion and PSD performance.

Our companding design composed of two parts. First, we derive the optimal companding function with a given segmentation point A and clipping value B . It is solving constraint optimization variational problem given in eqn. (9). According to Euler-Lagrange equation, the optimal companding function given in eqn.(11) is not related with the

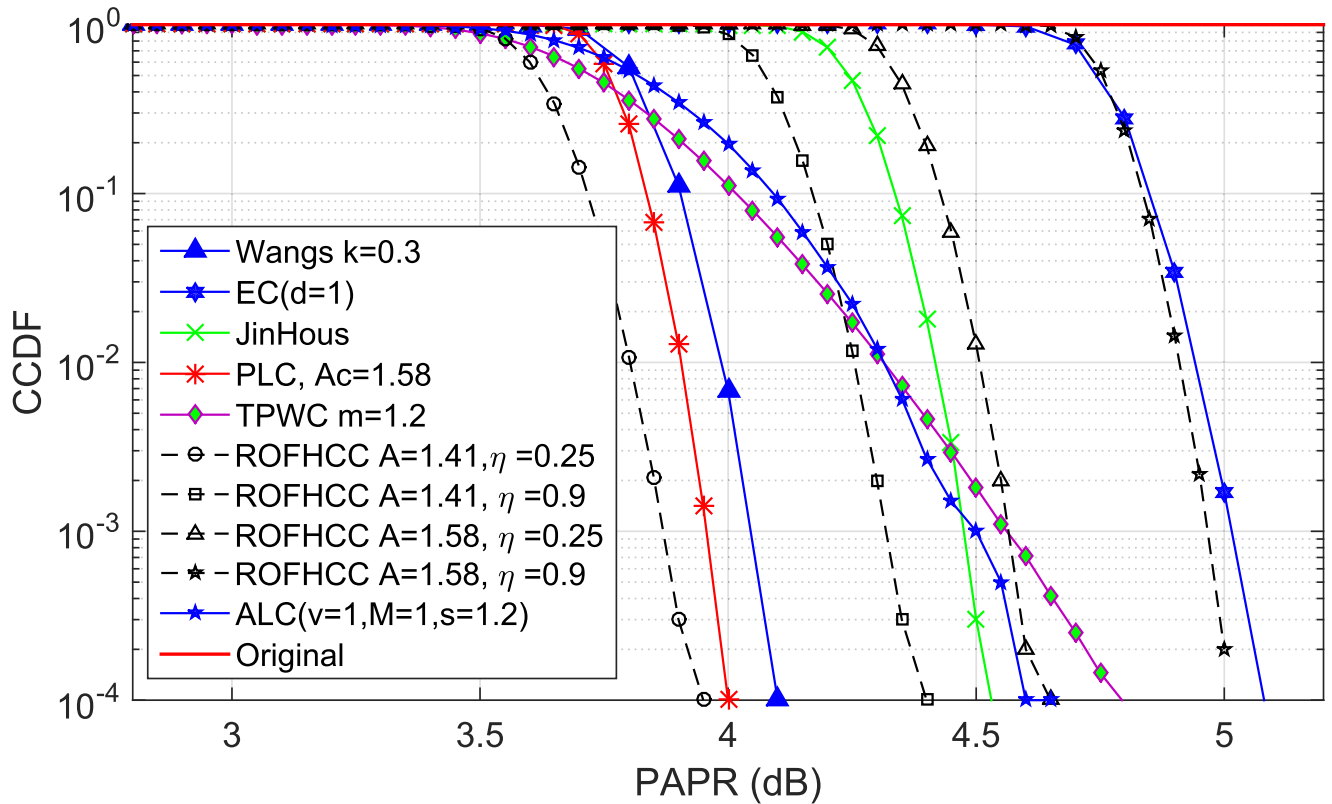


FIGURE 4. PAPR performance for different companding schemes.

TABLE 1. Some optimal values for k and B for different values of η and A .

η	k	B	A
0.25	1.0431	1.6538	1.58
0.5	1.0416	1.6622	
0.75	1.0376	1.6835	
0.25	1.0307	1.7357	1.68
0.5	1.0298	1.7423	
0.75	1.0276	1.7597	
0.25	1.0215	1.8212	1.78
0.5	1.0210	1.8262	
0.75	1.0198	1.8397	
0.25	1.0148	1.9099	1.88
0.5	1.0146	1.9135	
0.75	1.0139	1.9235	
0.25	1.0092	2.0197	2
0.5	1.0091	2.0221	
0.75	1.0089	2.0287	
0.25	1.0010	2.5025	2.5
0.5	1.0010	2.5028	
0.75	1.0010	2.5035	

PDF of the signal amplitudes. So the conclusion that with a determined segmentation point A and clipping value B , the optimal companding function is linear companding function is suited for new OFDM-based waveform candidates, such as filtered-OFDM, windowed-OFDM and circularly pulsed-shaped OFDM [21]–[24]. Second, we build a regularized constraint optimization problem to find the parameters for proposed companding scheme given in eqn. (42). For different OFDM-based waveform, the PDF of signal amplitudes

$f(x)$ might be different, but the design idea can be moved from OFDM systems to other OFDM-based waveform candidates.

IV. SIMULATION RESULTS

To verify the performance of the proposed companding scheme with respect to the PAPR, BER and PSD performance, simulation results are presented for OFDM systems. The number of subcarriers is chosen to be 256 with 4 times oversampling, while the modulation scheme is chosen as QPSK. We choose average signal power σ^2 to be 1.

When considering the passing of companded signals through a HPA, the input–output characteristics of the non-linear region are described by a solid state power amplifier (SSPA), which is also known as the Rapp model [25]. In our simulation, it presents only AM/AM conversion, which is expressed as

$$z(t) = \frac{y(t)}{\left\{ 1 + \left[\frac{y(t)}{A_{sat}} \right]^{2p} \right\}^{\frac{1}{2p}}}. \tag{43}$$

In eqn. (43), p ($p > 0$) is the shaping factor that controls the transition from the linear region to the saturation region. The variable A_{sat} represents the maximum value of the saturation region. The SSPA model assumes linear performance for low amplitudes of the input signal. Then, a transition toward a constant saturated output is observed. In our simulation, the shaping factor is chosen as 2 while the value of A_{sat} is

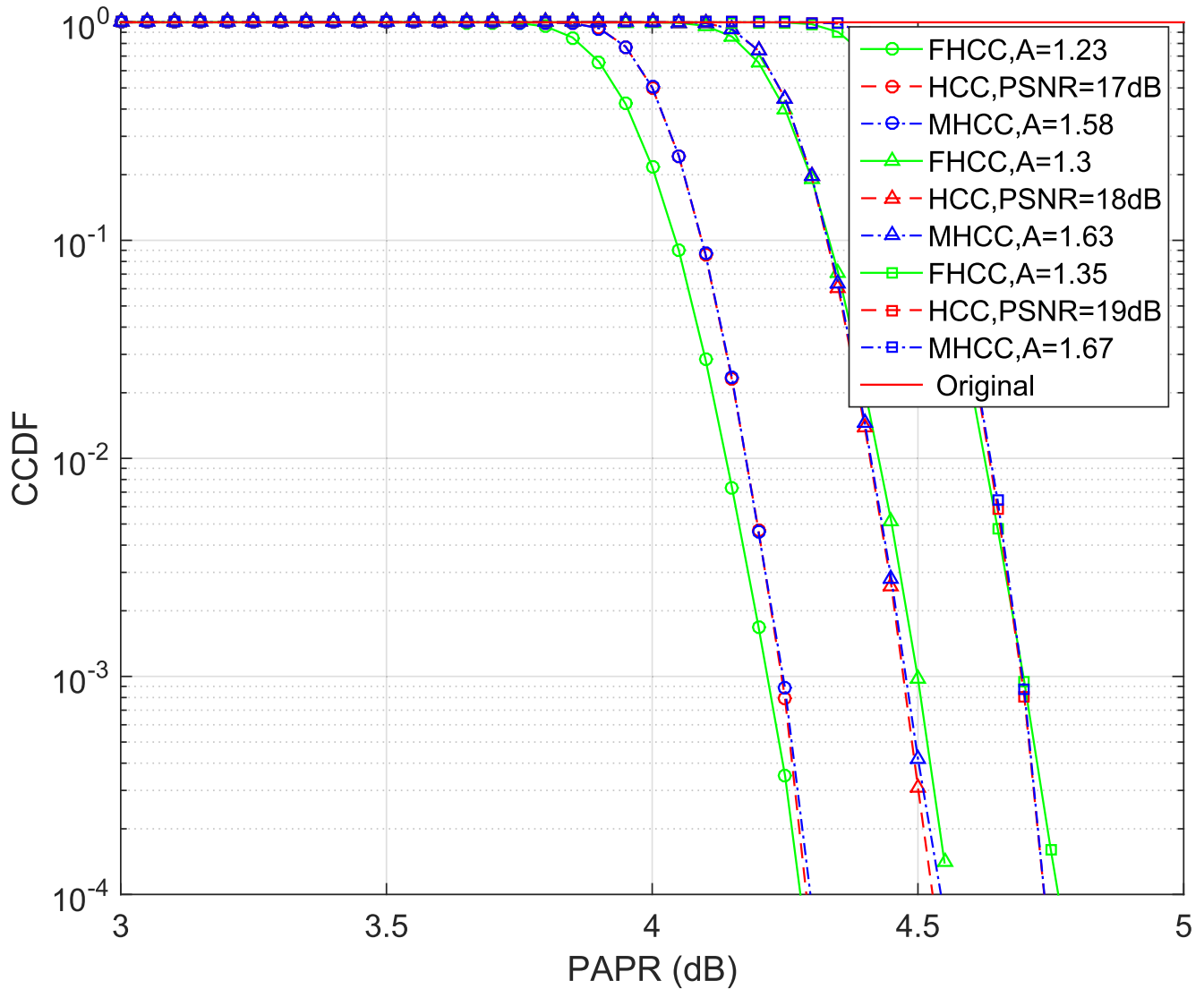


FIGURE 5. PAPR performance for HCC, FHCC and MHCC schemes.

set as 1.5. The proposed companding scheme was compared with TPWC ($m = 1.2$) [10], PLC scheme [11], EC ($d = 1$) scheme [14], JinHous Scheme [15], Wangs scheme [16] and ALC scheme [17].

Fig. 4 plots the simulated CCDFs of the PAPR for the original and companded signals using QPSK. The results illustrate that the ROFHCC scheme can significantly reduce the PAPR while simultaneously obtaining sharp drops in their CCDFs. Given that $CCDF = 10^{-4}$, the PAPR of the proposed companding scheme with $A = 1.41$, $\eta = 0.25$ is around 3.8 dB while the proposed companding scheme with $A = 1.41$, $\eta = 1.6$ is around 4.3 dB.

Fig. 5 shows the PAPR performance for HCC, MHCC and FHCC schemes. As shown in Fig. 5, the FHCC and MHCC schemes show good PAPR performance. For example, at $CCDF = 10^{-4}$, the PAPR is 4.2 dB for FHCC when $A = 1.23$ and for MHCC when $A = 1.58$; the PAPR is

4.5 dB for FHCC when $A = 1.3$ and for MHCC when $A = 1.63$; the PAPR is 4.8 dB for FHCC when $A = 1.35$ and for MHCC when $A = 1.67$.

The simulated BER versus E_b/N_0 curves for the original and companded signals using QPSK over an AWGN channel is presented in Fig. 6. It is observed that as the signal-to-noise ratio (SNR) increases, the ROFHCC scheme achieves better BER performance. Moreover, the performance of the proposed companding scheme is better than that of the referred schemes. For example, at a BER level of 10^{-4} for QPSK, the minimum required E_b/N_0 of ROFHCC scheme with $A = 1.41$, $\eta = 0.25$ is around 9.7 dB, which surpasses Wangs scheme ($k = 0.3$) 0.2 dB. Besides, the amount of BER improvement gradually increases when E_b/N_0 becomes larger. It is also found that the minimum required E_b/N_0 for ROFHCC scheme with $A = 1.41$, $\eta = 0.9$ is around 9.3 dB when $BER = 10^{-4}$, which surpasses ALC scheme 0.3 dB.

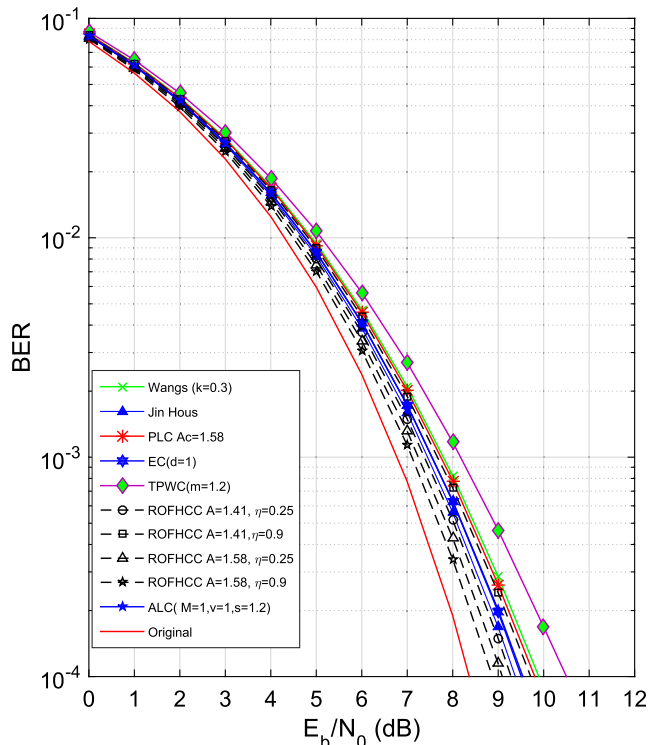


FIGURE 6. BER Performance for different companding schemes.

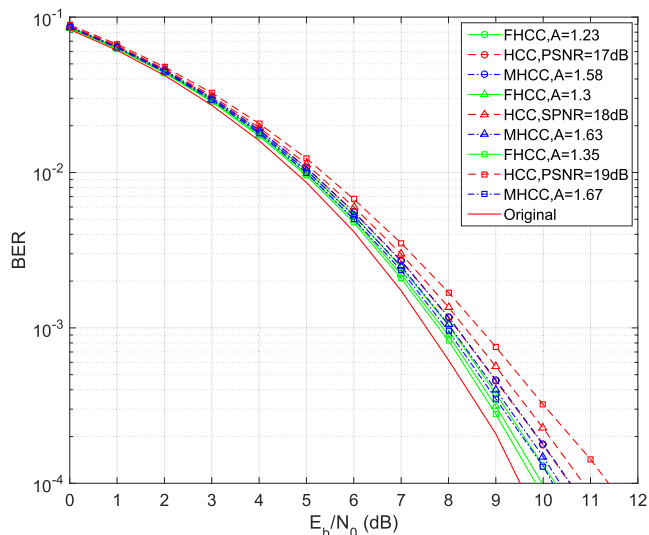


FIGURE 7. BER Performance for different HCC, FHCC and MHCC schemes with SSPA.

Moreover, at $BER = 10^{-4}$, the minimum required E_b/N_0 for ROFHCC scheme with $A = 1.58, \eta = 0.25$ is 9.1 dB, which surpasses EC ($d = 1$) scheme and TPWC ($m = 1.2$) scheme 0.5 dB and 1.4 dB, respectively.

Fig. 7 shows BER performance for HCC, MHCC and FHCC schemes over AWGN channel with SSPA. As shown in Fig. 7, the FHCC and MHCC schemes shows better BER performance than HCC scheme. For example, at $BER = 10^{-4}$, the minimum required E_b/N_0 for FHCC scheme with $A = 1.23$ is around 10.2 dB, which is around

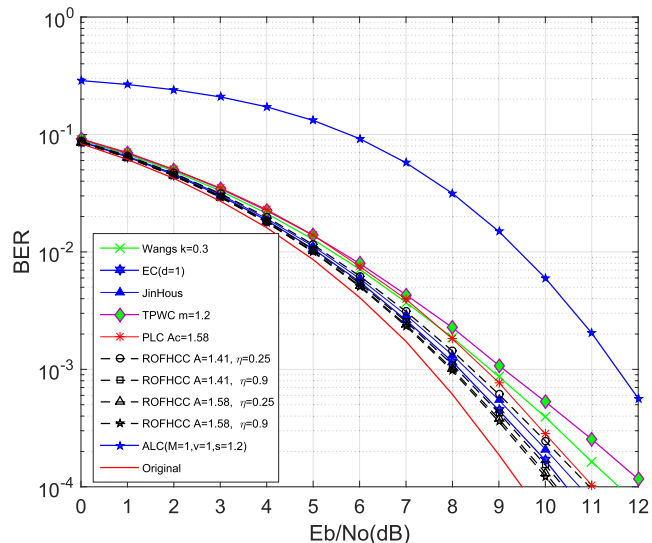


FIGURE 8. BER Performance for different companding schemes with SSPA.

TABLE 2. PSD performance for different companding schemes.

Companding Schemes	E_b/N_0 (dB), $BER=10^{-4}$		PAPR(dB) at CCDF= 10^{-4}
	AWGN (no SSPA)	AWGN (with SSPA)	
Proposed $A=1.41, \eta=0.25$	9.7	10.8	3.8
Proposed $A=1.41, \eta=0.9$	9.3	10.5	4.3
Proposed $A=1.58, \eta=0.25$	9.1	10.3	4.7
Proposed $A=1.58, \eta=0.9$	8.8	10.2	5
PLC, $A_c=1.58$	9.8	11	4.0
Wangs $k=0.3$	9.9	11.7	4.0
JinHous	9.4	10.7	4.3
ALC ($v=1, M=1, s=1.2$)	9.6	12.0	4.6
TPWC ($m=1.2$)	10.5	12.0	4.5
EC($d=1$)	9.6	10.6	4.7

1 dB lower than HCC scheme; the minimum required E_b/N_0 for MHCC scheme with $A = 1.58$ is around 10.5 dB, which is around 0.7 dB lower than HCC scheme; the minimum required E_b/N_0 for FHCC scheme with $A = 1.3$ is around 9.9 dB, which is around 1 dB lower than HCC scheme; the minimum required E_b/N_0 for MHCC scheme with $A = 1.63$ is around 10.2 dB, which is around 0.7 dB lower than HCC scheme; the minimum required E_b/N_0 for FHCC scheme with $A = 1.35$ is around 9.8dB, which is around 0.7 dB lower than HCC scheme.

Fig. 8 depicts the BER versus E_b/N_0 curves for companded signals using QPSK with the SSPA over AWGN channel. As observed, the BER performance of ROFHCC scheme is also robust enough with SSPA model. As an example, to achieve $BER = 10^{-4}$ in AWGN with SSPA, the minimum required E_b/N_0 for proposed scheme with $A = 1.41, \eta = 0.25$, PLC scheme ($A_c = 1.58$) and Wangs scheme are 10.8 dB, 11 dB and 11.7 dB, respectively. More simulation results are summarized in Table II, where we can see the effectiveness of the proposed companding scheme compared to the existing schemes in the literature.

The simulated PSD of companded signals is depicted in Fig. 9. As shown, combined with the PAPR performance figure in Fig. 4, for the same PAPR performance, the ROFHCC scheme has lower out-of-band (OOB) radiation of PSD than the referred companding schemes.

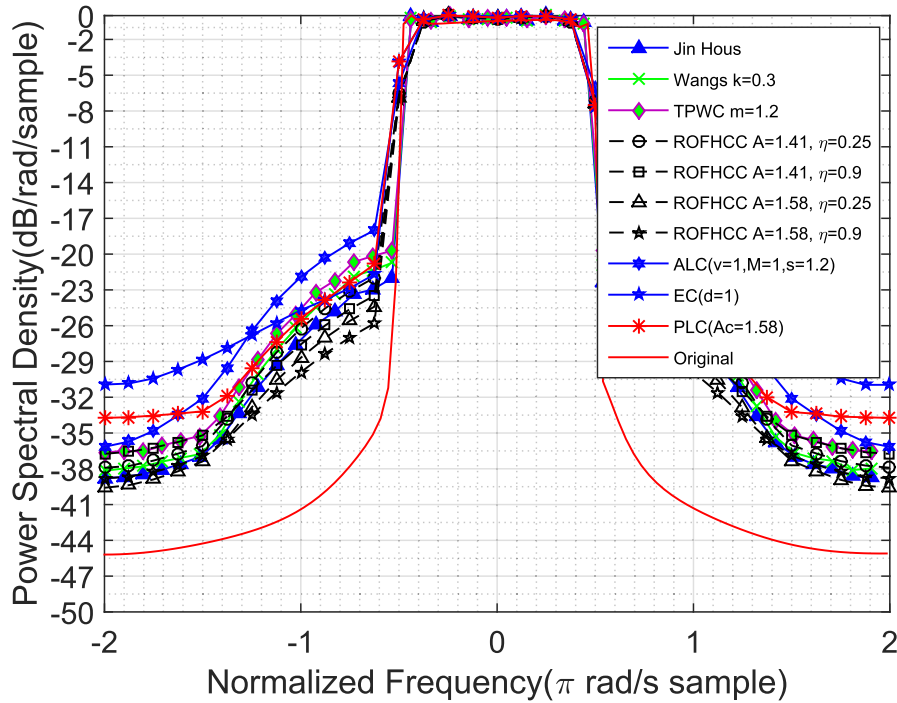


FIGURE 9. PSD performance for different companding schemes.

TABLE 3. Complexity Comparison for different Companding Schemes.

Compander	Additions	Multiplications	logarithm	square root	Exponentiation	Comparison
HCC	0	1	0	0	0	1
FHCC	0	1	0	0	0	1
MHCC	0	1	0	0	0	1
ROFHCC	0	1	0	0	0	1
EC	1	4	0	1	1	0
ALC	1	3	0	0	2	0
Wangs	3	3	0	1	1	1
JinHous	2	3	0	1	1	1
PLC	1	1	0	0	0	2
TPWC	1	2	0	0	0	1

Table III shows the complexity analysis for different companding schemes. The complexity analysis includes the times of additions, multiplications, logarithm, square root, exponentiation and comparison. As shown in Table III, ROFHCC, FHCC and MHCC scheme only costs 1 multiplications and 1 comparison. Hence, it has a complexity advantage over other companding schemes.

V. CONCLUSION

OFDM suffers from high PAPR problem, particularly in the mmWave spectrum which leads to carriers with a large number of OFDM sub-carriers. In this work, a low distortion companding scheme is proposed to reduce the PAPR of OFDM systems. When the signal amplitude is less than the given peak power amplitude, linear expanding function is used to enlarge the signal amplitude. When the signal amplitude is larger than the given peak amplitude, the signal amplitude will be restrained to a constant value. We determine

the parameters for the proposed companding function by solving a constraint optimization problem. The constraint condition is the average signal power constant before and after companding while the optimization goal is the combination of companding distortion and the continuity of companding function. Simulation results show that the proposed companding scheme shows better BER and PSD performance than referred companding scheme for the same PAPR performance. For example, when the average signal power is normalized to be 1, we choose both PAPR for ROFHCC scheme and ALC scheme as 4.6 dB, then we can find that at $BER = 10^{-4}$, the minimum required E_b/N_0 for ROFHCC scheme is around 0.5dB lower than ALC scheme.

APPENDIX A
EULER-LAGRANGE FUNCTION SOLVING

Considering that both the constraint equation and the optimization equation have only an unknown function in the first

term, the above optimization problem is rewritten as

$$F = \int_0^A [h(x) - x]^2 f(x) dx. \quad (44)$$

The constraint equation is rewritten as

$$\int_0^A h(x)^2 f(x) dx = \sigma^2 - \int_A^{+\infty} B^2 f(x) dx = C. \quad (45)$$

The optimization problem is simplified as

$$\begin{aligned} & \arg \min_{h(x) \in C_n} F, \\ & s.t. \int_0^A h(x)^2 f(x) dx = \sigma^2 - \int_A^{+\infty} B^2 f(x) dx = C. \end{aligned} \quad (46)$$

To solve the calculus of the variation problem with equality constraints, the optimization problem and the equality constraint need to be transformed into Lagrange form, as shown in eqn. (47)

$$\begin{aligned} L &= \int_0^A \{ [h(x) - x]^2 f(x) \} dx + \lambda \left[\int_0^A h^2(x) f(x) dx - C \right] \\ &= \int_0^A \{ [h(x) - x]^2 f(x) + \lambda h^2(x) f(x) \} dx - C\lambda. \end{aligned} \quad (47)$$

It is assumed that the integral part of L is $H(h, x)$, and

$$T(h, x) = \{ [h(x) - x]^2 f(x) + \lambda h^2(x) f(x) \}. \quad (48)$$

According to the Euler–Lagrange function,

$$\frac{\partial T}{\partial h} = 0. \quad (49)$$

Then,

$$h(x) = \frac{1}{1 + \lambda} x = kx. \quad (50)$$

APPENDIX B PROOF OF SUFFICIENCY OF Euler–Lagrange EQUATION

In fact, the Euler–Lagrange function is the necessary condition, so it is necessary to prove its sufficiency. This is equal to investigating the Jacobi condition and Weierstrass function.

First, the Jacobi function is investigated. The solution of the E-R function can be written as

$$y = kx. \quad (51)$$

Eqn. (51) can be regarded as a line beam with crossover point (0,0). The Jacobi function can be written as

$$\frac{\partial^2 H}{\partial h^2} u = 0, \quad (52)$$

where u is one of the solutions of the Euler–Lagrange equation. It is assumed to be $u = k_0x$. Therefore, for the Jacobi function

$$(2f + 2\lambda f) k_0x = 0, \quad (53)$$

only cross over point satisfy the Jacobi function. Thus, the Jacobi condition is satisfied.

Second, the Weierstrass function is investigated. We first calculate

$$p = \frac{dy}{dx} = k. \quad (54)$$

Thus, the Weierstrass function is

$$E = H(x, y) - H(x, y) - (k_0 - k) \times 0 = 0 \geq 0. \quad (55)$$

So the Weierstrass function is satisfied. Therefore, the sufficiency is satisfied.

APPENDIX C PROOF OF THE UNEQUATIONS

we assume $A = m\sigma^2$ ($m > 0$), then we obtain

$$\begin{aligned} G &= \sigma^2 - e^{-m^2} (m^2 \sigma^2 + \sigma^2) \\ &= \sigma^2 (1 - m^2 e^{-m^2} - e^{-m^2}). \end{aligned} \quad (56)$$

We suppose that

$$S = (1 - m^2 e^{-m^2} - e^{-m^2}), \quad (57)$$

then we obtain

$$\frac{\partial S}{\partial m} = 2me^{-m^2} - 2me^{-m^2} + 2m^3 e^{-m^2} > 0. \quad (58)$$

So we obtain S is monotonic increasing. This means

$$S > S(0) = 0. \quad (59)$$

So we prove that $(1 - m^2 e^{-m^2} - e^{-m^2}) > 0$.

REFERENCES

- [1] C. B. Barneto, T. Riihonen, M. Turunen, L. Anttila, M. Fleischer, K. Stadius, J. Ryynanen, and M. Valkama, "Full-duplex OFDM radar with LTE and 5G NR waveforms: Challenges, solutions, and measurements," *IEEE Trans. Microw. Theory Techn.*, vol. 67, no. 10, pp. 4042–4054, Oct. 2019.
- [2] Y. Rahmatallah and S. Mohan, "Peak-to-average power ratio reduction in OFDM systems: A survey and taxonomy," *IEEE Commun. Surveys Tuts.*, vol. 15, no. 4, pp. 1567–1592, 4th Quart., 2013.
- [3] M. Kozioł. (Jul. 2019). *5G's Waveform is a Battery Vampire*. [Online]. Available: <https://spectrum.ieee.org/telecom/wireless/5gs-waveform-is-a-battery-vampire>
- [4] A. S. Rajasekaran, M. Vameghestahbanati, M. Farsi, H. Yanikomeroglu, and H. Saeedi, "Resource allocation-based PAPR analysis in uplink SCMA-OFDM systems," *IEEE Access*, vol. 7, pp. 162803–162817, 2019.
- [5] W. Hu, "SLM-based ACO-OFDM VLC system with low-complexity minimum amplitude difference decoder," *Electron. Lett.*, vol. 54, no. 3, pp. 141–146, 2018.
- [6] Z. Zhou, L. Wang, and C. Hu, "Low-complexity PTS scheme for improving PAPR performance of OFDM systems," *IEEE Access*, vol. 7, pp. 131986–131994, 2019.
- [7] Y. Hori and H. Ochiai, "A new uplink multiple access based on OFDM with low PAPR, low latency, and high reliability," *IEEE Trans. Commun.*, vol. 66, no. 5, pp. 1996–2008, May 2018.

- [8] X. Huang, J. Lu, J. Zheng, K. B. Letaief, and J. Gu, "Companding transform for reduction in peak-to-average power ratio of OFDM signals," *IEEE Trans. Wireless Commun.*, vol. 3, no. 6, pp. 2030–2039, Nov. 2004.
- [9] S. A. Aburakhia, E. F. Badran, and D. A. E. Mohamed, "Linear companding transform for the reduction of peak-to-average power ratio of OFDM signals," *IEEE Trans. Broadcast.*, vol. 55, no. 1, pp. 155–160, Mar. 2009.
- [10] P. Yang and A. Hu, "Two-piecewise companding transform for PAPR reduction of OFDM signals," in *Proc. 7th Int. Wireless Commun. Mobile Comput. Conf.*, Jul. 2011, pp. 619–623.
- [11] M. Hu, Y. Li, W. Wang, and H. Zhang, "A piecewise linear companding transform for PAPR reduction of OFDM signals with companding distortion mitigation," *IEEE Trans. Broadcast.*, vol. 60, no. 3, pp. 532–539, Sep. 2014.
- [12] X. Wang, T. T. Tjhung, and C. S. Ng, "Reduction of peak-to-average power ratio of OFDM system using a companding technique," *IEEE Trans. Broadcast.*, vol. 45, no. 3, pp. 303–307, Sep. 1999.
- [13] Z. Xing, K. Liu, and Y. Liu, "Closed-form and analytical BER expression for OFDM system with μ -law companding operation," *China Commun.*, vol. 16, no. 7, pp. 61–69, Jul. 2019.
- [14] T. Jiang, Y. Yang, and Y.-H. Song, "Exponential companding technique for PAPR reduction in OFDM systems," *IEEE Trans. Broadcast.*, vol. 51, no. 2, pp. 244–248, Jun. 2005.
- [15] J. Hou, J. Ge, D. Zhai, and J. Li, "Peak-to-average power ratio reduction of OFDM signals with nonlinear companding scheme," *IEEE Trans. Broadcast.*, vol. 56, no. 2, pp. 258–262, Jun. 2010.
- [16] Y. Wang, L.-H. Wang, J.-H. Ge, and B. Ai, "An efficient nonlinear companding transform for reducing PAPR of OFDM signals," *IEEE Trans. Broadcast.*, vol. 58, no. 4, pp. 677–684, Dec. 2012.
- [17] B. Adebisi, K. Anoh, and K. M. Rabie, "Enhanced nonlinear companding scheme for reducing PAPR of OFDM systems," *IEEE Syst. J.*, vol. 13, no. 1, pp. 65–75, Mar. 2019.
- [18] V. Cuteanu and A. Isar, "PAPR reduction of OFDM signals using hybrid clipping-companding scheme with sigmoid functions," in *Proc. Int. Conf. Appl. Electron.*, Sep. 2011, pp. 1–4.
- [19] R. Raich, H. Qian, and G. T. Zhou, "Optimization of SNDR for amplitude-limited nonlinearities," *IEEE Trans. Commun.*, vol. 53, no. 11, pp. 1964–1972, Nov. 2005.
- [20] L. Daniel, *Calculus of Variations and Optimal Control Theory a Concise Introduction*. Princeton, NJ, USA: Princeton Univ. Press, 2013.
- [21] A. Nimr, M. Chafii, and G. P. Fettweis, "Unified low complexity radix-2 architectures for time and frequency-domain GFDM modem," *IEEE Circuits Syst. Mag.*, vol. 18, no. 4, pp. 18–31, 4th Quart., 2018.
- [22] J. Yli-Kaakinen, T. Levanen, A. Palin, M. Renfors, and M. Valkama, "Generalized fast-convolution-based filtered-OFDM: Techniques and application to 5G new radio," *IEEE Trans. Signal Process.*, vol. 68, pp. 1213–1228, 2020.
- [23] X. Zhang, L. Zhang, P. Xiao, D. Ma, J. Wei, and Y. Xin, "Mixed numerologies interference analysis and inter-numerology interference cancellation for windowed OFDM systems," *IEEE Trans. Veh. Technol.*, vol. 67, no. 8, pp. 7047–7061, Aug. 2018.
- [24] H. Chen, J. Hua, J. Wen, K. Zhou, J. Li, D. Wang, and X. You, "Uplink interference analysis of F-OFDM systems under non-ideal synchronization," *IEEE Trans. Veh. Technol.*, vol. 69, no. 12, pp. 15500–15517, Dec. 2020.
- [25] P. Banelli, G. Baruffa, and S. Cacopardi, "Effects of HPA nonlinearity on frequency multiplexed OFDM signals," *IEEE Trans. Broadcast.*, vol. 47, no. 2, pp. 123–136, Jun. 2001.



ZHITONG XING received the B.S. degree from the Chongqing University of Posts and Telecommunication, Chongqing, China, in 2011 and 2015, respectively. He is currently pursuing the Ph.D. degree in communications and information systems with the School of Electronic Engineering, Beijing University of Posts and Telecommunications. His research interest includes signal processing for wireless communications.



Hoc/mesh networks, and heterogeneous wireless networks.

KAIMING LIU (Member, IEEE) received the B.S. and Ph.D. degrees in communication engineering from the Beijing University of Posts and Telecommunications (BUPT), in 2001 and 2006, respectively. He is currently an Associate Professor with the School of Electronic Engineering, BUPT, and the Director of the Wireless Smart Communications and Networking (WSCN) Laboratory. His current research interests include broadband wireless communication networks, wireless Ad



Radio (NR) solutions. His research interests include wireless technology solutions aimed towards 5G and beyond cellular networks, including non-orthogonal multiple access solutions.

ADITYA S. RAJASEKARAN (Member, IEEE) received the B.Eng. (Hons.) and M.Eng. degrees in systems and computer engineering from Carleton University, Ottawa, ON, Canada, in 2014 and 2017, respectively, where he is currently pursuing the Ph.D. degree in systems and computer engineering. He is also with Ericsson Canada, where he has been working as a Software Developer since 2014. He is also involved in baseband physical layer development work for Ericsson's 5G New



Technology Society. He has been a one of the most frequent tutorial presenters in the leading international IEEE conferences. He has had extensive collaboration with industry which resulted in 37 granted patents (plus more than a dozen applied). From 2012 to 2016, he led one of the largest academic-industrial collaborative research projects on pre-standards 5G wireless, sponsored by the Ontario Government and the industry. He has served as the general chair and a technical program chair for several major international IEEE conferences. He is also serving as the Chair of the Steering Board for the IEEE's flagship wireless conference, Wireless Communications and Networking Conference (WCNC).

HALIM YANIKOMEROĞLU (Fellow, IEEE) is currently a Professor with Carleton University, Canada. He has supervised 26 Ph.D. students (all completed with theses). His research interest includes many aspects of communications technologies with emphasis on wireless networks. He is also a Fellow of the Engineering Institute of Canada (EIC) and the Canadian Academy of Engineering, and a Distinguished Speaker of the IEEE Communications Society and the IEEE Vehicular



In 1995, he started his second postdoctoral in the Broadband Mobile Laboratory, Department of System and Computer Engineering, Carleton University, Ottawa, ON, Canada. Since July 1997, he has been a Professor with the Wireless Communication Center, College of Telecommunication Engineering, BUPT, where he is involved in the development of next-generation cellular systems, wireless LAN, Bluetooth application for data transmission, EMC design strategies for high speed digital system, and EMI and EMS measuring sites with low cost and high performance.

YUANAN LIU (Member, IEEE) received the B.E., M.Eng., and Ph.D. degrees in electrical engineering from the University of Electronic Science and Technology of China, Chengdu, China, in 1984, 1989, and 1992, respectively. In 1984, he joined the 26th Institute of Electronic Ministry of China to develop the inertia navigating system. In 1992, he began his first postdoctoral position in the EMC Laboratory, Beijing University of Posts and Telecommunications (BUPT), Beijing, China.

...